Influence of excimer laser surface melting on anodising of AA2024-T351 alloy

Influence of excimer laser surface melting on anodizing of AA2024-T351 alloy

Z. Aburas*, F. Viejo, Y. Yuan, Z. Liu, P. Skeldon and G.E. Thompson

Corrosion and Protection Centre, School of Materials
The University of Manchester, M60 1QD, UK
**Corresponding author. Tel: +44(0)161-3062920; Fax: +44(0)161-3064865*
e-mail: zakria.aburas@postgrad.manchester.ac.uk

Summary
This paper presents a potential application of laser surface melting (LSM) as a pre-treatment technique prior to a conventional anodizing for aluminium alloys. A KrF excimer laser, with wavelength of 248 nm and pulse width of 13 ns, was used for surface melting of AA2024-T351 alloy, with variation of laser fluence and number of pulses received per unit area. After laser treatment, the specimens were anodized with a constant voltage of 12 V, in 0.46 M sulphuric acid for 12 min. Materials characterization, in terms of surface morphology, microstructural and compositional homogenization, phase transformation, and measurement of residual stress, was performed using FEG-SEM/EDX, TEM/HRTEM and XRD. The corrosion behaviour was evaluated based on ASTM G34-01 EXCO test and by electrochemical polarization. The results showed that the excimer laser surface melting of the alloy significantly improved the corrosion performance following anodizing compared with the alloy anodized without prior laser treatment.

Keywords: anodizing; laser surface melting; excimer laser; corrosion; aluminium.

Introduction

AA2024-T351 alloy is widely used in the aerospace industry due to its optimized mechanical properties, damage tolerance performance and low density. However, as with all 2xxx aluminium alloys, the main alloying elements are Cu and Mg which, together with Fe, Mn and Si as impurities, usually form various intermetallic particles with dimensions up to tens of microns and population densities ranging from 3×10^5 to 1×10^6 /cm^2 [1,2]. This results in a severe reduction of localized corrosion resistance of the alloys due to the formation of microgalvanic cells, when they are exposed in chloride containing environments [3]. Therefore, such surfaces often require protection against corrosion, which is usually accomplished by anodizing, followed by application of organic coatings [4]. However, the presence of intermetallic particles is well recognised in causing a reduction in efficiency of the anodizing process, modifying the film morphology and generating of flaws in the film [5]. By focussing on such defects, more effective corrosion control scheme will be available to enhance applications of aluminium alloys as infrastructure and transport materials.

It is well known that laser surface melting (LSM) melts a thin layer of the alloy surface, with consequent modification of the microstructure and chemical homogenisation by refinement and dissolution of precipitates and inclusions, as well as redistribution of the alloying elements [6]. This results in an enhancement of corrosion and wear properties of the melted surface [7-10]. Excimer laser radiation sources in the UV range of wavelength and nanosecond pulse width result extremely fast cooling rates up to 10^{11} Ks^{-1} [11], which favours the formation of amorphous or rapidly solidified microstructures that are largely free of segregation and intermetallic precipitates [12,13]. Recent work has demonstrated that LSM of AA2024-T351 alloy with an excimer laser produced a relatively uniform melted layer with a melt depth up to 5-7 μm, and eliminated large sized intermetallic particles and dispersoids in

the original alloy matrix [14]. Therefore, it is expected that LSM prior to anodizing may provide significant benefits in terms of improved anodizing behaviour and hence corrosion performance. Consequently, the aim of the present work is to investigate the influence of excimer laser surface melting on anodizing of AA 2024-T351 alloy. Microstructural characterization and corrosion performance of the alloy with and without laser treatment and followed by anodizing have been considered.

Experimental Procedure

Test material: Commercial AA2024-T351 alloy was supplied in the form of 10 mm plate; the chemical composition of the alloy, analyzed by IncoTest, was 4.30 Cu, 1.41 Mg, 0.61 Mn, 0.17 Fe, 0.04 Si, balance Al (wt.%).

Laser Surface Melting: Prior to laser treatment, the specimens were ground to 1200 SiC grit finish, and then cleaned with distilled water and ethanol. LSM was conducted in the ambient environment, using a 80 W Lumonics KrF excimer laser with a wavelength of 248 nm and pulse width of 13 ns. The spot size of the incident laser beam on the specimen surface was 4.0 mm x 1.75 mm and the laser fluence was fixed at 6.0 J/cm^2. The number of pulses per unit area was varied from 10, through 25 to 50, to evaluate their influence on the microstructural and corrosion properties of the melted layers. In order to cover a sufficiently large area, the LSM process was performed with an overlap ratio of 33%.

Anodizing Treatment: After LSM, the as-processed specimens were anodized in stirred 0.46 M sulphuric acid electrolyte at room temperature using a constant voltage of 12 V for 12 min; the anodized specimens were sealed in boiling deionised water for 30 min. For comparison, the as-received alloy was also anodized and sealed under the same conditions to provide a reference.

Corrosion Evaluation: In order to evaluate the electrochemical properties of various treated-specimens, potentiodynamic polarisation was performed in deaerated 0.1 M NaCl solution at 22 ºC, using a Solartron 1286 potentiostat and a conventional three-electrode cell employing a platinized titanium counter electrode and a saturated calomel reference electrode (SCE). The solutions were deaerated by purging with nitrogen for 60 min. The specimens, as-processed, were then immersed in the solution for 60 min to stabilize the open circuit potential. Anodic polarization curves were determined at a sweep rate of 0.167 mV/s. Purging with nitrogen was continued throughout the test. In addition, immersion tests based on ASTM G34-01 EXCO were carried out in a naturally aerated solution containing 4 M NaCl, 0.5 M KNO_3 and 0.1 M HNO_3 at a temperature of 25 ºC for 6 h.

Microstructural Characterisation: Material characterisation in terms of surface morphology, microstructural and compositional uniformity, and phase transformations were undertaken using high-resolution transmission electron microscopy (HRTEM), high angle annular dark field (HAADF) in the scanning-transmission (STEM) mode, energy-dispersive X-ray spectroscopy (EDS), scanning electron microscopy (SEM), using a Philips XL30 FEG-SEM and EVO50 microscopes both equipped with EDS, and low-angle X-ray diffraction (XRD). In addition, measurement of residual stress was conducted on the laser-treated and as-received specimens with a Proto iXRD stress measurement system using copper as an anode (Cu Kα 1.5406 Å) and nickel as a filter.

Results and Discussion

Microstructural Characterisation: Figure 1 shows a typical microstructure of the as-received AA2024-T351 alloy, containing intermetallic particles distributed randomly in the aluminium

matrix. Combination of the results from XRD and SEM/EDS analyses revealed that the intermetallic particles were mainly roughly spherical Al_2CuMg (S-phase), of approximate size 5-10 μm, and the irregularly shaped Al(Cu,Fe,Mn) phase of approximate size 10-20 μm.

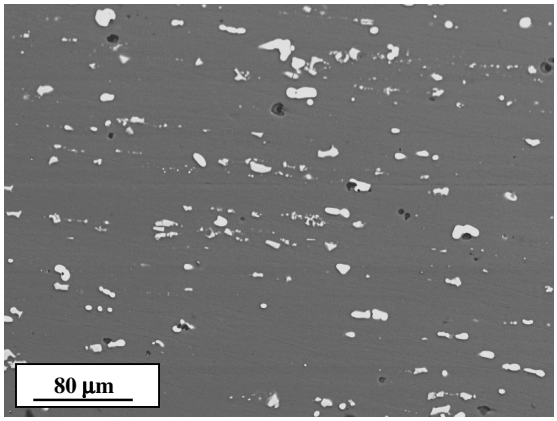

Figure 1. SEM micrograph of the as-received AA2024-T351 alloy.

After LSM, the surface showed a wave-like or rippled morphology with a succession of valleys and hills along the laser scan direction (Figure 2a). This morphology has been previously reported as typical of excimer laser radiations [15]. Further, the surface roughness tended to increase when the number of laser pulses was increased. From cross sectional examination of the laser-treated specimens, as shown in Figure 2b, it is evident that the melted layer was relatively uniform in depth. Increasing the number of laser pulses from 10 to 50 resulted in increased depth of the melted layers from about 5 μm to 10–14 μm. Observation of the microstructural changes revealed that large constituent intermetallic particles within the melted layer had dissolved, and had partially melted at the interface between laser-treated layer and the bulk alloy. Fine dispersoids in the original alloy matrix within the melted layer had dissolved.

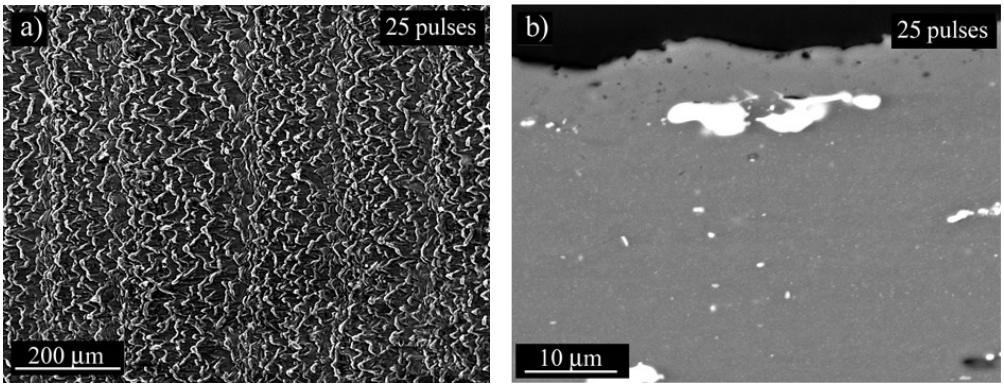

Figure 2. SEM micrographs of laser-melted morphology by 25 pulses, a) plain view and b) cross-section.

XRD patterns, as shown in Figure 3, confirmed that increasing the number of laser pulses enhanced the dissolution of the intermetallic phases. When the surface was treated by 10 pulses, the S-phase (Al_2CuMg) and the other large intermetallic particles like Al(Cu,Fe,Mn) were still present but with lower intensity. The presence of such phases might be due to the relatively shallow melt depth which allowed phases in the bulk alloy beneath the melt pool to

be probed by XRD, although low-angle XRD was used. In addition, incomplete dissolution of the phases might also contribute to the XRD peaks. When the number of laser pulses was increased to 25 and 50, no intermetallic particles were evident, indicating a complete dissolution/removal of various intermetallic particles within the melted surface.

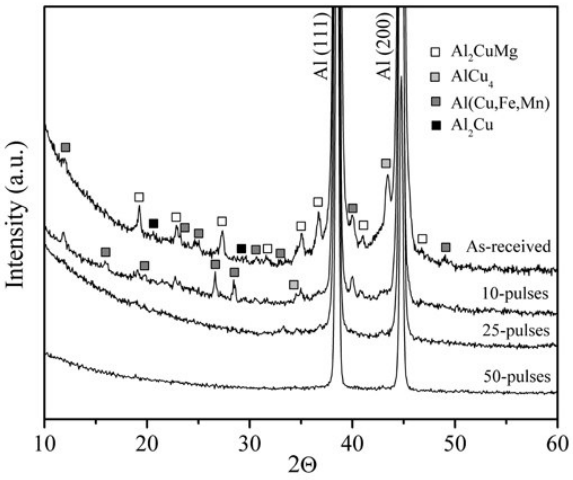

Figure 3. XRD patterns of AA2024-T351 before and after LSM.

In addition, in the interfacial region between the melted layer and the alloy substrate, fine single or double layers, containing mainly copper, along with manganese and iron, were observed for the specimen treated by 10 pulses (Figure 4). Such layers might arise from the melted particles that form a solute rich liquid, which is not fully dispersed [16], due to insufficient time for diffusion in each single laser pulse duration (13 ns). Nevertheless, by increasing the number of laser pulses, these solute segregation bands were less prevalent. A similar finding was also reported in our work on excimer laser melting of AA2050-T8 alloy [17].

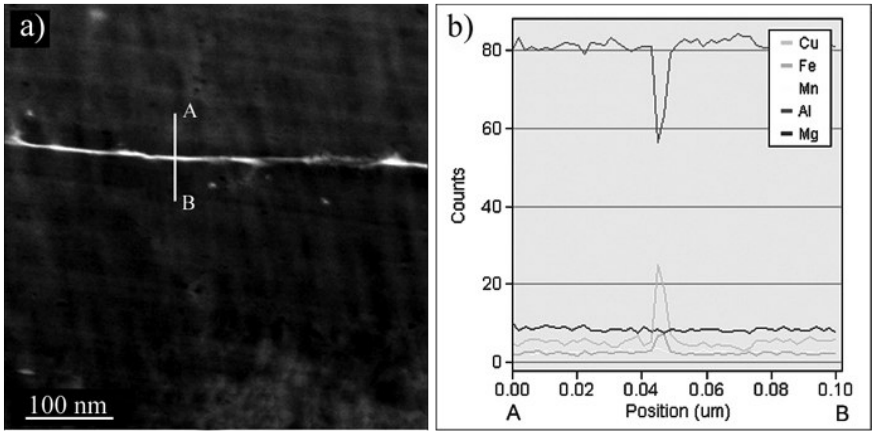

Figure 4. HADDF image (a) and elemental profile (b) of interface between the melted layer and substrate for the specimen treated by 10 pulses.

Anodizing: Figure 5 shows the current density/time behaviour recorded during the anodizing at 12 V for the laser-melted specimens, as well as the as-received alloy. It revealed an initial surge in current density followed by a decrease to a minimum value and an increase to a

steady current density. This is a typical response for anodizing aluminium alloys in acid electrolytes; the initial stage is normally related to non-uniform film growth, with relatively uniform thickening of the porous anodic film in the steady current density region [18]. Figure 5 also presented a significant decrease steady of the current density from 2.5 mA/cm^2 for the as-received AA2024-T351, to 0.9 mA/cm^2 for laser-treated with 50 pulses. Furthermore, the current density in the steady regions decreased with an increase in the number of laser pulses. This responses suggest that LSM increased the efficiency of growth of the anodic film on the AA2024-T351 alloy, due to the dissolution of intermetallic phases in the near surface alloy regions.

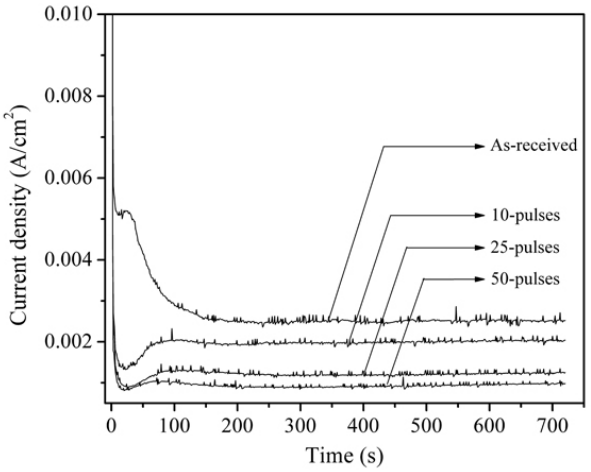

Figure 5. Current density response during anodizing process for the as-received and laser-melted specimens.

Corrosion Evaluation

a) Anodic Polarization. Figure 6 shows the anodic polarization curves determined for the as-received and laser-treated specimens in deaerated 0.1 M NaCl solution. It is evident that the excimer laser surface melting significantly reduced the passive current density by more than two orders of magnitude.

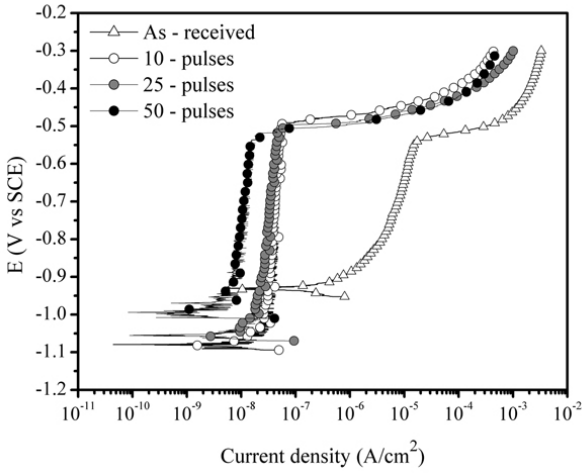

Figure 6. Anodic polarization curves for as-received and laser-treated specimens after immersion in deaerated 0.1 M NaCl solution.

Such improvement of corrosion performance is considered to be associated with the dissolution/removal of the large intermetallic particles including Al_2CuMg (S-phase) and Al(Cu,Fe,Mn) phases, as a result of extreme high cooling rates produced by excimer laser radiation. Further, the higher the number of laser pulses, favouring the complete removal of such phases, therefore, led to further shifts of the passive current density toward lower values.

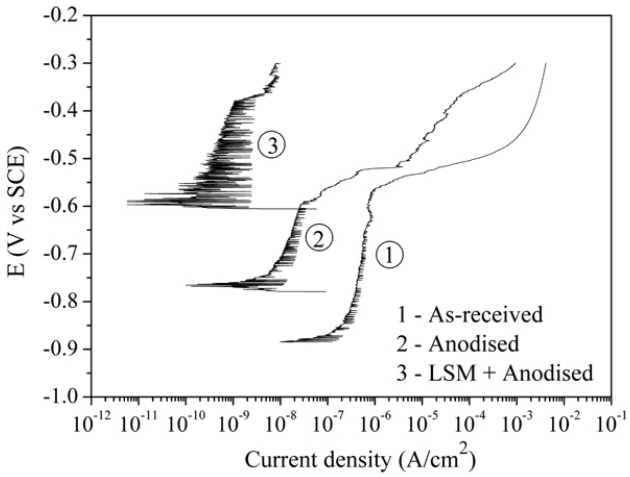

Figure 7. Anodic polarization curves for as-received, LSM treated (25-pulses) and LSM treated + anodizing specimens after immersion in deaerated 0.1 M NaCl solution.

The influence of the excimer laser melting as a pre-treatment prior to anodizing on corrosion performance is shown in Figure 7. Clearly, excimer laser surface melting resulted in a marked reduction in the passive current density, by about two and four orders of magnitude compared with the as-received alloy with and without anodizing, respectively. From Figure 7, it is evident that the corrosion and pitting potential values had increased for the LSM-anodized specimens. Table 1 summaries the electrochemical data determined from the anodic polarization measurement. It was concluded that corrosion performance of the AA2024-T351 alloy in NaCl solution was greatly improved by the following factors: *i)* the use of excimer LSM; *ii)* the increased number of laser pulses; but overall *iii)* the use of excimer LSM as pre-treatment technique prior to anodizing.

Table 1. Electrochemical data determined from the anodic polarization curves.

Treatment		Ecorr (V)	Epit (V)	Passive current density (A/cm^2)
As-received		-0.88	-0.51	1.0E-6
LSM	**10-pulses**	-1.09	-0.50	3.0E-8
	25-pulses	-1.05	-0.50	2.0E-8
	50-pulses	-0.99	-0.52	0.8E-8
Anodizing	**As-received**	-0.76	-0.61	2.0E-8
	10-pulses	-0.74	-0.60	0.8E-9
	25-pulses	-0.60	-0.37	0.3E-9
	50-pulses	-0.56	-0.31	0.2E-9

b) EXCO immersion test. Figure 8 displays cross sections of the as-received, laser-treated and LSM followed by anodized specimens after the EXCO immersion test for 6 h. As expected,

the as-received specimen exhibited severe intergranular attack and exfoliation of individual grains (Figure 8a). After LSM, the sample treated by 10 pulses showed a slightly improvement in corrosion resistance, but intergranular attack of the bulk alloy revealed. More importantly, delamination of the laser-melted layer from the bulk alloy was evident. With increasing number of the laser pulses up to 50, further improvement was obtained but still with the occurrence of potential delamination. After anodizing, a significant improvement was observed when a 50-pulse treatment was applied as the pre-treatment, with no delamination evident.

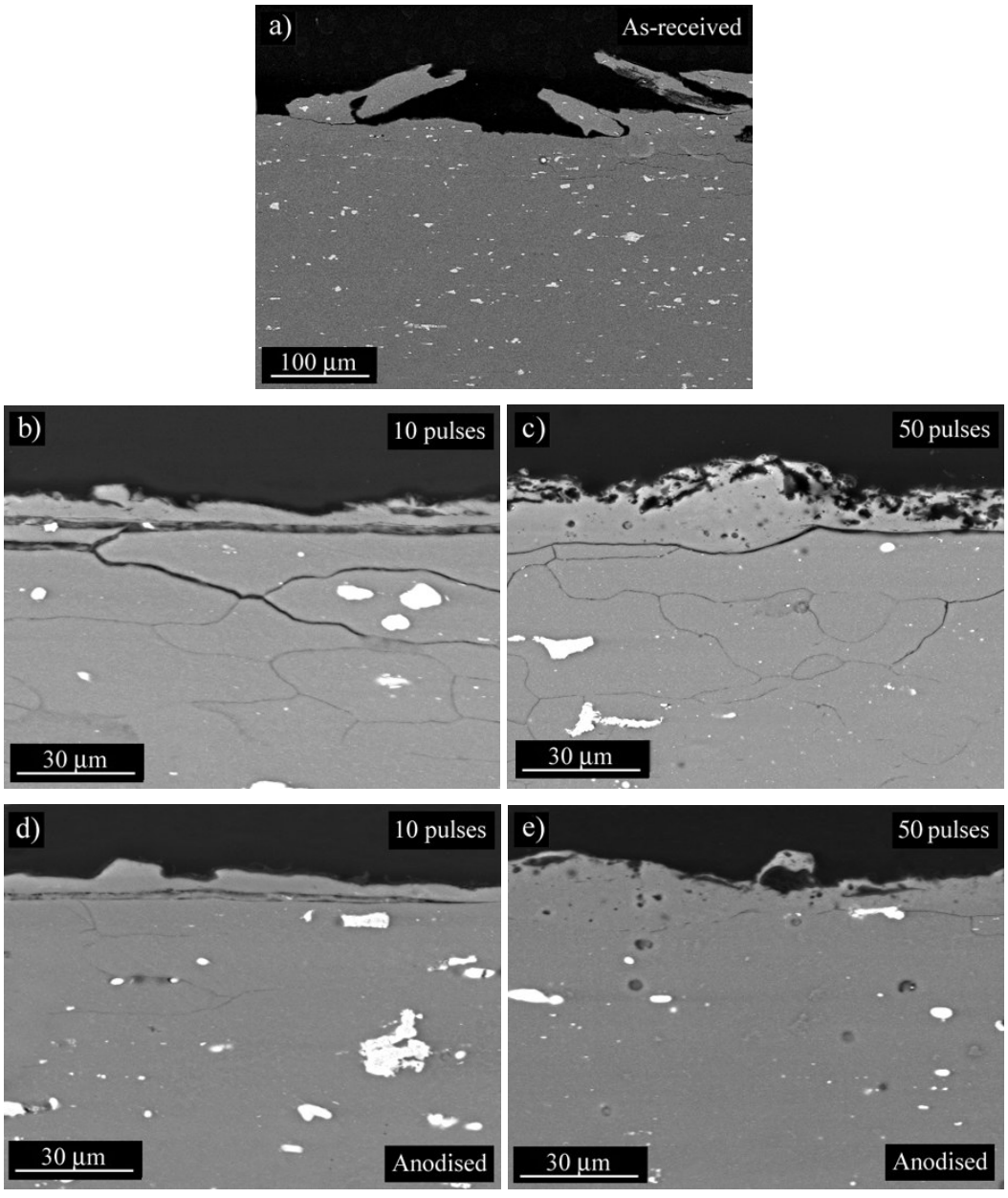

Figure 8. SEM micrographs of the cross-sections of the specimens after EXCO test for 6 h.

Since the delamination occurred along the interfacial region between the melted layer and the substrate, it might suggest that the presence of the copper-rich layers at the interface as mentioned earlier might attribute to the causes. These layers of high Cu and Fe contents are

cathodic respect to the matrix alloy; thus, galvanic attack is favoured along the melted layer/bulk material interface once the electrolyte in contact with this region through defects in the melted layers. The consequence led to delamination of the melted layers. Additionally, it was observed that this delamination became less pronounced for the specimens treated by an increased number of laser pulses. This is due to the increasing number of laser pulses limiting the development of solute segregation bands and enhanced dispersion of the solute elements within the α-Al solid solution.

Table 2. Surface residual stress measurements for as-received and laser-treated specimens.

Material	Residual Stress (MPa)	
	0º (X - direction)	**90º (Y- direction)**
As-received	-20.5± 15.7	-27.7 ± 16.3
LSM-10 pulses	50.2 ± 84.3	74.7 ± 99.1
LSM-25 pulses	98.6 ± 22.5	115.9 ± 25.3
LSM-50 pulses	73.0 ± 19.8	97.8 ± 19.5

In order to assist further understanding of the delamination behaviour, residual stress measurements at the near-surface of the as-received and laser-treated specimens were conducted. Residual stress in the surface layers (10 - 15 μm) of metallic materials can be determined by measuring the changes in the lattice parameters of the matrix alloy [6]. From the experimental results, as shown in Table 2, it can be deduced that excimer laser surface melting of AA2024-T351 alloy changed the sign of the stress in the surface layer from compressive to tensile. Further, the increase of the number of laser pulses on the level of residual tensile stress was not conclusive. The change of compressive stress to tensile stress by excimer laser surface melting observed in the work was inconsistent with the data by Badekas and Panagopoulus [6,19], who observed a change of residual stress in the surface of an Al-4 wt% Cu alloy from tensile to compressive as a result of excimer LSM. It was suggested that the presence of the tensile stress, in combination with the copper-rich layers at the interface between the melted layer and the substrate, may result in a stress-related corrosion mechanism, leading to delamination of the melted layers.

Conclusions

1. Excimer LSM of AA2024-T351 produced a relatively uniform surface layer, with a melt depth from 5 μm to about 10-12 μm, and complete dissolution/removal of the intermetallic particles. Formation of a copper-rich layer at the interface became less prevalent with increasing number of laser pulses.

2. Excimer LSM of AA2024-T351 alloy improved the localised corrosion resistance of the alloy, by reducing the passive current density more than two orders of magnitude. The higher the number of laser pulses, the better the corrosion performance was obtained.

3. Excimer LSM, used as a pre-treatment prior to conventional anodizing, greatly improved the anodizing performance in acid media, by increasing growth efficiency of the anodic film, due to the dissolution of intermetallic phases in the near surface.

4. Anodized AA 2024-T351 with LSM as a pre-treatment further reduced the passive current density by about two and four orders of magnitude compared with the as-received alloy with and without anodizing respectively. Further, increased corrosion and pitting potentials were recorded for the LSM-anodized specimens.

5. Laser surface melted specimens revealed different degrees of delamination of the laser-melted layer, which might be attributed to *i)* the presence of copper-rich layers at the melted layer/bulk alloy interface, favouring the formation of microgalvanic cells and, *ii)* the introduction of tensile residual stress in the melted region after LSM treatment, leading to stress-related corrosion mechanism. However, the delamination was significantly reduced for the specimen treated by 50 pulses, especially after anodizing. Therefore, it was believed that such problems might be solved by appropriate selection of the number of laser pulses during excimer LSM, in combination of prolonged time period of anodizing.

Outlook

Further work is in progress to gain insight into the influence of laser surface melting on the anodizing treatments of aluminium alloys, in terms of morphology of growth and development of the anodic porous film, with paying attention to the relationship between protective layer resultant and their corrosion performance.

References

[1] R.G. Buchheit, R.P. Grant, P.F. Hiava, B. Mckenzie and G.L. Zender, Journal of the Electrochemical Society, **1997**, *144***,** 2621.

[2] P. Schmutz and G.S. Frankel, Journal of the Electrochemical Society, **1998**, *145***,** 2285.

[3] R. Ambat, N.N. Aung, and W.Zhou., Journal of Applied Electrochemistry, **2000**, 30, 865.

[4] B.J. Conolly, and J.R. Scully, Corrosion, **2005**, *61*, 1145.

[5] P. Campestrini, E.P.M. van Westing, H.W. van Rooijen and J.H.W. de Wit, Corrosion Science, **2000**, *42*, 1853.

[6] H. Badekas, A. Koutsomichalis and C. Panagopoulos, Surface and Coatings Technology, **1988**, *34*, 365.

[7] K.G. Watkins, M.A. McMahon and W.M. Steen, Materials Science & Engineering A, **1997**, *231*, 55.

[8] Z. Liu, P.H. Chong, P. Skeldon, P.A. Hilton, J.T. Spencer, B. Quayle, Surface and Coatings Technology, **2006**. *200*, 5514.

[9] Z. Liu, P.H. Chong, A.N. Butt, P. Skeldon, G.E. Thompson, Applied Surface Science, **2005**, *247*, 294.

[10] R.F. Li, M.G.S. Ferreira, A. Almeida, R. Vilar, K.G. Watkins, M.A. McMahon and W.M. Steen, Surface and Coatings Technology, **1996**, *81*, 290.

[11] M.L. Autric, J. Perrais and G. Barreau, Proceeding of SPIE Conference, **2000**, 742-749.

[12] T.M. Yue, L.J. Yan, C.P. Chan, C.F. Dong, H.C. Man, G.K.H. Pang, Surface and Coatings Technology, **2004**, *179,* 158.

[13] C.P. Chan, T.M. Yue and H.C. Man, Material Science and Technology, **2002**, *18*, 575.

[14] Y. Yuan, Z. Aburas, T. Hashimoto, Z. Liu, P. Skeldon and G.E. Thompson, Electrochemical Society Transactions, **2008**, *11*, 49.

[15] A. Koutsomichalis, L. Saettas, H. Badekas, Journal of Materials Science, **1994**, *29*, 6543.

[16] P. Ryan, P.B. Pragnell, Materials Science and Engineering A, **2008**, *479*, 65.

[17] F. Viejo, Z. Liu, Y. Yuan, A. E. Coy, G. E. Thompson, P. Skeldon, T. Hashimoto, M. C. Merino and T. Warner, Proceeding of ICAA 11, **2008**. Submitted.

[18] M. Curioni, M. Saenz de Miera, P. Skeldon, G.E. Thompson and J. Ferguson, Journal of the Electrochemical Society, **2008**, *155*, 387.

[19] C. Panagopoulos and A. Michaelides, Journal of Materials Science, **1992**, *27*, 1280.